

Inhibition Effect of Phthalocyaninatocopper(II) and 4-Tetranitro(phthalocyaninato)copper(II) Inhibitors for Protection of Aluminium in Acidic Media

Thabo Pasha¹, Gobeng R. Monama¹, Mpitloane J. Hato^{1,*}, Thabiso C. Maponya¹, Mamookgo E. Makhatha², Kabelo E. Ramohlola¹, Kerileng M. Molapo³, Kwena D. Modibane^{1,**}, Mary S. Thomas¹

¹ Department of Chemistry, School of Physical and Mineral Sciences, Faculty of Science and Agriculture, University of Limpopo (Turfloop Campus), Polokwane, Sovenga 0727, South Africa

² Department of Metallurgy, School of Mining, Metallurgy and Chemical Engineering, Faculty of Engineering and Built Environment, University of Johannesburg (Doorfontein Campus), Johannesburg 2001, South Africa

³ Department of Chemistry, Faculty of Natural Science, University of the Western Cape (Bellville Campus), Cape Town 7535, South Africa

*E-mails: kwena.modibane@ul.ac.za; mpitloane.hato@ul.ac.za

Received: 4 January 2018 / Accepted: 3 October 2018 / Published: 30 November 2018

The inhibition effect of phthalocyaninatocopper(II) (CuPc) and 4-tetranitro(phthalocyaninato)copper(II) (TNCuPc) on aluminium in 1 mol/L HCl was investigated by electrochemical techniques. The CuPc and TNCuPc inhibitors were synthesized and confirmed by using X-ray diffraction (XRD), Fourier transform infrared (FTIR), simultaneous thermal analysis (STA, thermogravimetric analysis (TGA)/differential scanning calorimetry (DSC)) and ultraviolet-visible spectroscopy (UV-vis). The XRD, UV-vis and FTIR analyses showed successful formation of CuPc and TNCuPc inhibitors. The thermal stability of CuPc increased upon the introduction of NO₂ group in the peripheral position as indicative of the formation of TNCuPc. The potentiodynamic polarization (PDP) curves of aluminium in the corrosive environment of HCl in the presence and absence of CuPc and TNCuPc compounds demonstrated that both cathodic and anodic processes of Al corrosion were suppressed. The Nyquist plots of electrochemical impedance spectroscopy (EIS) expressed mainly as a capacitive loop with different concentrations of CuPc and TNCuPc. The inhibition efficiency of these inhibitors increased with increase in inhibitor concentration, and their inhibition efficiencies in the same concentration decreased in the order of CuPc > TNCuPc according to PDP and EIS results due to a steric hindrance.

Keywords: Phthalocyaninatocopper(II); 4-tetranitro(phthalocyaninato)copper(II); corrosion inhibitor; aluminium; electrochemical measurements

1. INTRODUCTION

Metals and their metallic alloys find extensive use in our daily life and form part of human body system [1, 2]. For example, aluminium (Al) is a light metal, a good electric conductor and has been used in a variety of electronic applications [3]. However, one of the challenging problems in the usage of this metal is the need to protect it from corrosion attack. It has been shown that corrosion attack can be protected by using different methods such as upgrading materials; blending of production fluids, process control and corrosion chemical inhibition [3-5]. Amongst these methods, the corrosion chemical inhibition is reported to be the best method in the prevention of destruction or degradation of metal surfaces in corrosive media due to economic and practical usage [6-8]. The search for an efficient corrosion inhibitor is of paramount importance and as a fundamental progressive step in this quest; it has been found that the use of organometallic compounds is one of the most practicable ways of protecting metals from corrosion [9-11]. This is due to π – electron systems and the presence of highly electronegative atoms such as O, N, S and P [12, 13].

Metallophthalocyanines (MPcs) are organometallic complexes with planar molecules with 8 N-atoms in a macrocyclic nucleus entailing an extended conjugated 18 π – electron systems and aromatic rings [14-19]. Recently, attention has been paid to the use of phthalocyanines as potential corrosion inhibitors for different metals [17-19]. This is due to their planarity and the size of the molecular volume, their adsorption onto metal surface and enhancement in the surface coverage, thus efficient corrosion inhibition potentials [14]. In addition, MPcs have efficient corrosion inhibition properties because they are cost effective, easily synthesized, thermally stable and chemically noble [14, 18]. Valle-Quitana and co-workers [19] carried out corrosion inhibition studies using CuPc as an inhibitor for 1018 carbon steel in 0.5 M H₂SO₄. It was found that the CuPc acted as a good corrosion inhibitor for carbon steel, with its efficiency increasing with the concentration. In another study, CuPc was investigated as an effective inhibitor for high strength low alloy (HSLA) steel in 16% HCl [20]. A number of literature reports indicated that corrosion studies of Al employing organic substances are performed in acidic and basic media [21-24]. However, solubility and aggregation are other important properties that can also affect the adsorption and corrosion inhibition properties of MPcs on metals [14, 19, 25]. MPcs solubility in different solvents mainly depends on the substituent groups or coordinated ligand [26]. It has been reported that inhibitors that are completely soluble in the medium of interest exhibit higher inhibition efficiency [14, 26].

In this study, we intend to exploit a new aspect associated with the corrosion protection efficiency by introducing the nitro groups on the peripheral position of the CuPc, which we hypothesized to significantly enhance the adsorption capacity of the inhibitor on the aluminium metal. The chemical structures of phthalocyanines containing Cu and N are shown in Scheme 1. To the best of our knowledge, the use of CuPc and 4-tetranitro copper(II)phthalocyanine (TNCuPc) as corrosion inhibitors for Al metal sheet in HCl environment has not reported to date. The corrosion inhibition behavior of CuPc and TNCuPc inhibitors for Al metal in 1 M HCl solution was investigated by potentiodynamic polarization (PDP) and electrochemical impedance spectroscopy (EIS) techniques as part of our contribution in the quest for an inhibitor which does not only possess good inhibitive efficiency but also eco-friendly and can be synthesized with ease.

2. EXPERIMENTAL SECTION

2.1. Materials

Copper nitrate trihydrate ($\text{Cu}(\text{NO}_3)_2 \cdot 3\text{H}_2\text{O}$), trimesic acid, 1,3,5-benzenetricarboxylic acid (H_3BTC) and tetrabutylammonium percholate (TBAP) were purchased from Sigma Aldrich, South Africa. Phthalimide, 32% hydrochloric acid (HCl), methanol, nitrobenzene, ethanol, nitric acid (HNO_3) and sulphuric acid (H_2SO_4) were purchased from Rochelle Chemicals. Ammonium heptamolybdate ($(\text{NH}_4)_6\text{Mo}_7\text{O}_{24}$) and urea ($\text{CH}_4\text{N}_2\text{O}$) were purchased from uniLAB.

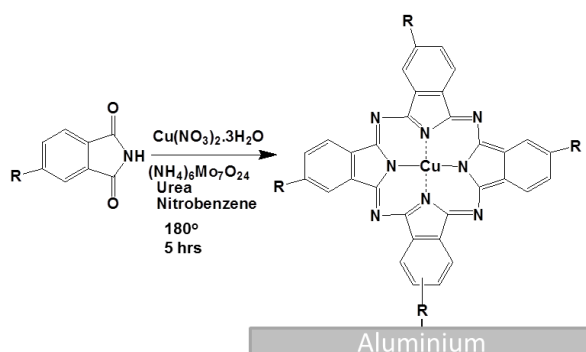
2.2. Methods

2.2.1. Synthesis of Phthalocyaninatocopper(II) and 4-tetranitro(phthalocyaninato)copper(II)

Phthalocyaninatocopper(II)(CuPc) used as corrosion inhibitor was synthesized by modifying the procedure described by Arici et al. [27]. Under a blanket of nitrogen, a mixture of phthalimide

(3.00 g, 0.0204 mol) in the presence of excess urea (3.00 g, 0.0500 mol), ammonium heptamolybdate (0.0800g, 0.0687 mmol) and copper nitrate (1.40 g, 0.0058 mol) in nitrobenzene (15.00 mL) was refluxed at 180°C for 5 hours with constant stirring. For purification, the product was finely ground and washed with ethanol three times. Ultraviolet-visible (UV-vis) (H_2SO_4): λ_{max} (log ϵ); 790 nm (5.11), 709nm (4.74), 448nm (4.62). Fourier transform infrared (FTIR): $\nu_{\text{max}}/\text{cm}^{-1}$; 3084 (Ar-H), 1609 (C=C), 1468 (C=C); 904, 880, 783, 781, 742 (Pc skeletal).

Synthesis and purification of 4-tetranitro(*phthalocyaninato*)copper(II) (TNCuPc) was done as outlined for CuPc, whereby 4-nitrophthalimide was used instead of phthalimide according to the reported method for preparation of phthalocyanine inhibitor [28] aiming to achieve improved corrosion inhibition efficiency towards aluminium metal. Briefly, Scheme 1. a mixture of 4-nitrophthalimide (3.00 g, 0.0156 mol) in the presence of excess urea (3.00 g, 0.0500 mol), ammonium heptamolybdate (0.0800g, 0.0687 mmol) and copper nitrate (1.40 g, 0.0058 mol) in nitrobenzene (15.00 mL) was refluxed for 5 hours at 180°C to give a target compound. The product was washed with ethanol and dried at 110°C , giving a yield of 2.64g (70 %) and melting point $>300^\circ\text{C}$. UV-vis (H_2SO_4): λ_{max} (log ϵ); 763nm (4.67), 739nm (4.65), 668nm (3.86), 418nm (4.02). FTIR: $\nu_{\text{max}}/\text{cm}^{-1}$; 3475 (Ar-H), 1601 (C=C), 1521 (N-O), 1337 (N-O); 910, 727, 755 (Pc skeletal).



Scheme 1. Preparation of phthalocyaninatocopper(II) (R=H) and 4-tetranitro(phthalocyaninato)copper(II) (R=NO₂) on Al sheet.

2.2.2. Characterization Techniques

The UV-vis spectra were obtained at room temperature in the wavelength region 200–900 nm employing a Varian Cary 300 UV-vis-NIR spectrophotometer. The X-ray diffraction (XRD Phillips PW 1830, CuK α radiation, $\lambda = 1.5406 \text{ \AA}$) was used to obtain the structure of the synthesized inhibitors. The successful synthesis of inhibitors was confirmed using the Spectrum II FTIR spectrometer (Perkin-Elmer). The spectra were recorded at room temperature in the wavenumber ranging between 450 and 4000 cm^{-1} at a minimum of 32 scans and a resolution of 4 cm^{-1} . The thermal stability of the CuPc and TNCuPc inhibitors was investigated using simultaneous thermal analysis (STA, thermogravimetric analysis (TGA) and differential scanning calorimetry (DSC)) (Perkin Elmer 6000). The weight of the samples ranged between 1 to 4 mg. The samples were heated from 30-500 $^{\circ}\text{C}$ at a heating rate of 20 $^{\circ}\text{C}\cdot\text{min}^{-1}$ under N_2 environment.

2.2.3. Electrochemical Measurements

Electrochemical measurements were achieved using Bio-Logic SP150 potentiostat working station which employed a three electrode cell namely, Ag/AgCl reference electrode (RE), platinum counter electrode (CE) and Al metal (1 cm^2) working electrode (WE) in the presence and absence of corrosion inhibitor concentrations. Potentiodynamic polarization studies were done at the scanning range between -0.250 and +0.250 mV at 1.0 mV/s constant sweep rate on the open circuit potential. The anodic and cathodic polarization curves were obtained when stabilization was accomplished after the WE was immersed in the test solution for 30 min. EIS measurements were done using 100 kHz to 10 MHz frequency range with 10 mV peak to peak, using AC signal at corrosion potential, E_{corr} . From EIS analysis, the values of the double layer capacitance, C_{dl} , and the charge transfer resistance, R_{ct} , were obtained. Furthermore, the anodic Tafel slope (b_a), the cathodic Tafel slope (b_c) as well as the corrosion current density (i_{corr}) were determined from the Tafel extrapolation method. Moreover, the percentage inhibition efficiency (%IE) were calculated with the help of the (Eq. 1) [29]:

$$\%IE_{PDP} = \left(\frac{i_{\text{corr}}^0 - i_{\text{corr}}^i}{i_{\text{corr}}^0} \right) \times 100 \quad (1)$$

where i_{corr}^0 and i_{corr}^i represent corrosion current density in absence (no protection) and the presence of inhibitors, respectively.

3. RESULTS AND DISCUSSION

3.1. Structural Properties

The XRD patterns of CuPc and TNCuPc inhibitors are presented in Fig. 1(a). The patterns of CuPc are similar to the one reported by Zongo et al. [30], suggesting a cubic structure of phthalocyanine. Moreover, a number of sharp diffraction peaks appearing at $2\theta = 5.7, 6.9$ and 9.1° corresponding to Miller indices (100), (110) and (111), respectively, are observed. These sharp peaks indicate highly crystalline structure [27, 31]. However, the diffraction peaks of TNCuPc possessed a decrease and

broadening patterns at $2\theta = 13.0, 14.5$ and 27.2° . This behaviour suggests a large crystal size of the CuPc upon introduction of the nitro groups at the periphery with amorphous character [30, 32, 33].

As demonstrated in Fig. 1(b), the successful synthesis of CuPc and TNCuPc inhibitors was further confirmed with FTIR in the region between $400\text{--}4500\text{ cm}^{-1}$. The peaks observed at ~ 3283 and 1720 cm^{-1} correspond to the N-H and C=O vibrations of the phthalimide, respectively [33]. Interestingly, these vibrations disappeared after conversion into both CuPc and TNCuPc, indicating the successful synthesis of metallophthalocyanine [34]. The vibrational peaks observed between 700 and 1000 cm^{-1} are typically due to phthalocyanines skeletal vibrations Mingyi Zhang and others, ‘Hierarchical Nanostructures of Copper (II) Phthalocyanine on Electrospun TiO₂ Nanofibers: Controllable Solvothermal-Fabrication and Enhanced Visible Photocatalytic Properties’, *ACS Applied Materials & Interfaces*, 2011, 369–77.. The characteristic of NO₂ stretch was observed at around 1350 and 1450 cm^{-1} , which is a substituent in the synthesized TNCuPc. The observable peaks at 3049 and 2910 cm^{-1} for CuPc are attributed to the symmetric C-H stretching in the ring and in the alkyl group, respectively [27]. The peak around 1609 cm^{-1} is due to C=C deformation of macro cycle ring in pyrrole and at around 1506 cm^{-1} is due to the C=N stretching. For isoindole, C-C stretching appeared at 1428 and 1332 cm^{-1} . At around $909, 882$ and 728 cm^{-1} is the appearance of the C-H bending. However, the peaks at around $1284, 1162$ and 1070 cm^{-1} are associated with C-N stretching in isoindole, C-N in plane bending, and C-H in plane bending, respectively [27, 30, 32, 33]. TNCuPc also showed strongest peaks of NO₂ group at 1334 and 1525 cm^{-1} on the phthalocyanine ring [32].

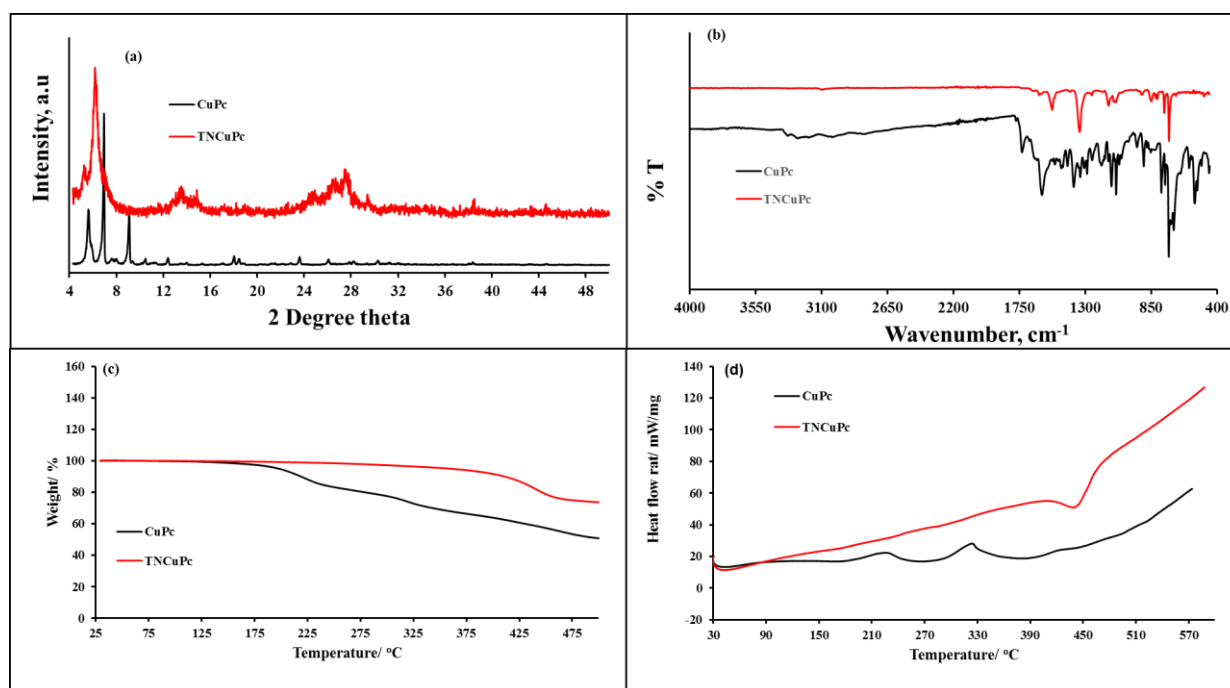


Figure 1. (a) XRD, (b) FTIR, (c) TGA, and (d) DSC of CuPc and TNCuPc inhibitors

Parts (c) and (d) of Fig. 1 show TGA and DSC curves of CuPc and TNCuPc inhibitors. The weight loss in TGA corresponds to the change in transition phase in the DSC curve. At the initial stage,

the weight loss is observed and due to the evaporation of water [36]. The TGA curves of CuPc shows three degradation steps between 180 and 294 and 330 as well as 400 °C, corresponding to the loss of benzimidazole moiety of the macromolecule and the oxidative degradation of phthalocyanine moiety, respectively [37]. As presented in Fig. 1(d), these peaks are also observable as melting transitions in the DSC curves. It is interesting to note that the introduction of NO₂ groups on the periphery of the CuPc improved the thermal stability of the TNCuPc inhibitor. The high thermal stability may be due to the stabilizing effect of NO₂ associated with the electron density acting onto the structure and blocking of Cu diffusion typically for Pcs [38]. A single degradation step is also observed at around 400 °C, which corresponds to the oxidative degradation of TNCuPc Zhang and others.. A single endothermic peak corresponding to the peak on the TGA is also noticeable in DSC curve of the TNCuPc.

Fig. 2(a) shows the UV-vis spectroscopic results of CuPc and TNCuPc dissolved in H₂SO₄. The spectra for the CuPc and TNCuPc displayed an intense Q absorption band in the 720-780 nm region of the visible range and a B band between 300-400 nm in the UV region. Both the Q and B bands are known to arise from $\pi-\pi^*$ transitions originating from the phthalocyanine ligand, and are assigned to the $6eg \rightarrow 2a1u$ transition for the Q-band and the $6eg \rightarrow 4a2u$ for the B-band A G Sharpe, 'Norgan Ic Ch Em Istry', 24 (1981), 1981.. The maximum wavelength values of the Q bands for all the CuPc and TNCuPc inhibitors are consistent with the data presented by Cong and co-workers Fang Di Cong and others, 'The Control of Phthalocyanine Properties through Nitro-Group Electronic Effect', *Spectrochimica Acta - Part A: Molecular and Biomolecular Spectroscopy*, 62.1-3 (2005), 394-97 <<https://doi.org/10.1016/j.saa.2005.01.006>>., and is indicative of the presence of phthalocyanine in the composite. Nonetheless, the TNCuPc shows a broader and a slightly blue-shifted Q-band A. V. Ziminov and others, 'Photoluminescence of Nitro-Substituted Europium (III) Phthalocyanines', *Semiconductors*, 44.8 (2010), 1070-73 <<https://doi.org/10.1134/S1063782610080208>>. relative to the MPcs. The unusual Q-band broadening and split may be due to the effect of the nature of solvent used Introduction Phthalocyanines, Spectrophotometer Unicam Uv, and Perkin Elmer Fluorescence Mpf-, '50 Years of Chemistry in Opole Octacarboxyphthalocyanines – Compounds of Interesting Spectral , Photochemical and Catalytic Properties 50 Years of Chemistry in Opole', 2014, 4-7.. In addition, the stronger intermolecular interactions lead to a higher degree of aggregation causing the replacement of the typical monomer Q-band structure by two broader bands and a blue shifted absorption band R Litrán and others, 'Trapping Copper Phthalocyanine in a Silica Sono-Xerogel', *Journal of Sol-Gel Science and Technology*, 8.1-3 (1997), 985-90 <<http://www.scopus.com/inward/record.url?eid=2-s2.0-0030646613&partnerID=40&md5=3f663d6248e333fd6df79778a8acaf56>>.. The TNCuPc inhibitor comprises both B- and Q-bands. The B-band of these phthalocyanines appears between 315-352 nm, and the Q-band was observed between 600-750 nm where the blue colour actually absorbs [27]. These bands arise from $\pi-\pi^*$ transitions and this can be inferred from the four frontier orbitals (HOMO and LUMO orbitals) [35]. Furthermore, two splitting absorption bands are observed around 630 and 710 nm, which is likely due to the vibronic coupling in the excited state [35]. As shown in Fig. 2(b), the Beer-Lambert's law was obeyed for the compound containing concentrations ranging from 0 to 5 ppm. The absorptivity coefficient of CuPc from Beer's law was found to be $\log \epsilon$ of 5.11 at 790 nm corresponding to the reported one [27]. On the other hand, the TNCuPc possessed the split absorbance with $\log \epsilon$ of 4.67 and 4.65 at 763 and 739 nm, respectively. These $\log \epsilon$ values also show that there are a number of

molecules interacting with light which will enhance the inhibition efficiency of the inhibitor on the aluminium metal [42].

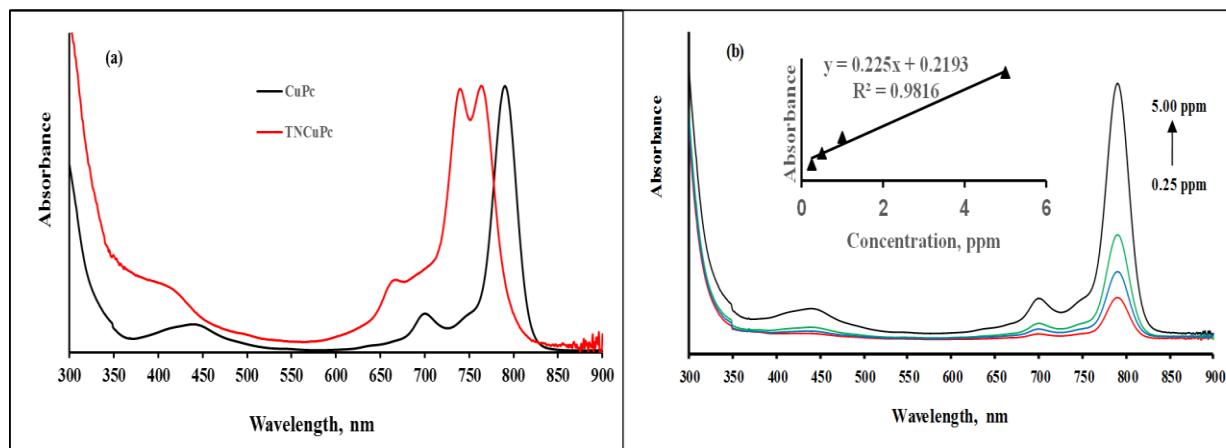


Figure 2. (a) UV-vis spectra of CuPc and TNCuPc in H_2SO_4 (~10 ppm), and (b) UV-vis spectra of CuPc at different concentration 0 to 5 ppm. Inset: concentration dependence of CuPc.

3.2. Electrochemical Analysis

3.2.1. Potentiodynamic Polarization (PDP)

Fig. 3 presents polarization curves for aluminium metal in the absence and presence of different concentrations of CuPc and TNCuPc inhibitors in 1 M HCl studied at room temperature and PDP parameters are listed in Table 1. It can be seen from the figure that the polarization curves are shifted towards lower corrosion current density regions upon the addition of various inhibitors relative to the blank solution (uninhibited). This behavior indicates the formation of protective film of the inhibitors on the Al metal surface and reduction in the rate of anodic dissolution of the metal [14]. The similarity in the polarization behavior of both CuPc and TNCuPc inhibitors indicates a similar inhibition mechanism. It was also noticeable that the addition of CuPc (Fig. 3(a)) and TNCuPc (Fig. 3 (b)) inhibitors did not affect to any significant degree neither the E_{corr} nor the i_{corr} values. However, they increased the passive current density (i_{pas}) and passivation potential (E_{pas}). As a result, the E_{corr} value for the uninhibited solution was -535.6 mV, and with the addition of inhibitors this value was around -498.7 and -515.2 mV for CuPc and TNCuPc, respectively at 40 ppm. The i_{corr} slightly decreased from 1.94 down to 0.091 and 0.26 mA/cm², 40 ppm CuPc and TNCuPc, respectively, and the lowest value obtained was brought about by the addition of 80 ppm in both inhibitors. The difference of greater than 85 mV between the corrosion potential values of the blank and the inhibited solutions suggest either an anodic or cathodic inhibitor type while that of less than 85 mV signifies a mixed-type [43, 44].

On the other hand, E_{pas} value for the blank solution was 465.4 mV. Nonetheless, the value decreased when both CuPc and TNCuPc inhibitors were introduced obtaining the lowest values of -

321.8 and -333.9 mV, respectively at 80 ppm. Correspondingly, the i_{pas} value of the blank is 4.68 mA/cm². Upon addition of CuPc and TNCuPc inhibitors, the i_{pas} decreased by increasing the concentration of the inhibitor obtaining the lowest values of 1.74 and 2.25 mA/cm² at 80 ppm. From these observations, it could be concluded that the addition of phthalocyanine inhibitors decreased the corrosion rate of Al metal in acidic medium by improving the passive film properties. It can be seen in Table 1 that b_a and b_c values change with the concentration of CuPc and TNCuPc inhibitors. The change in Tafel slope values in both inhibited and uninhibited solution can be used to identify the inhibition mechanism (anodic, cathodic or mixed-type) for aluminium metal, the concentration of the electrolyte, the composition of the working electrode, charge transfer coefficient as well as the scanning rate [45]. In another study [46], the change in b_a value for mild steel in acidic medium at different concentrations of caffeic acid inhibitor was reported. The authors attributed the change in b_a values to the possible occurrence of the redox complexation process, which involved ferrous and ferric complexes of the inhibitor, which was also affected by the concentration of the inhibitor and the pH of the medium. In our study, the overall magnitude of the difference between anodic and cathodic Tafel slope values in comparison to the blank system showed that the inhibition potential of the studied CuPc and TNCuPc inhibitors are cathodic-dominating since the changes in cathodic Tafel slope values are more significant than the anodic Tafel slope values [47, 48]. Furthermore, it can be seen that both CuPc and TNCuPc can act as effective inhibitors in 1 M HCl for aluminium and the inhibition efficiency decreases in the order of CuPc > TNCuPc at the 40 ppm concentration, as 95.3, and 86%, respectively. The highest 98% inhibition efficiency of CuPc at 80 ppm indicates an excellent inhibition. The increase in %IE with increase concentration suggests that the inhibitors are adsorbed onto to the surface of the Al metal surface [49].

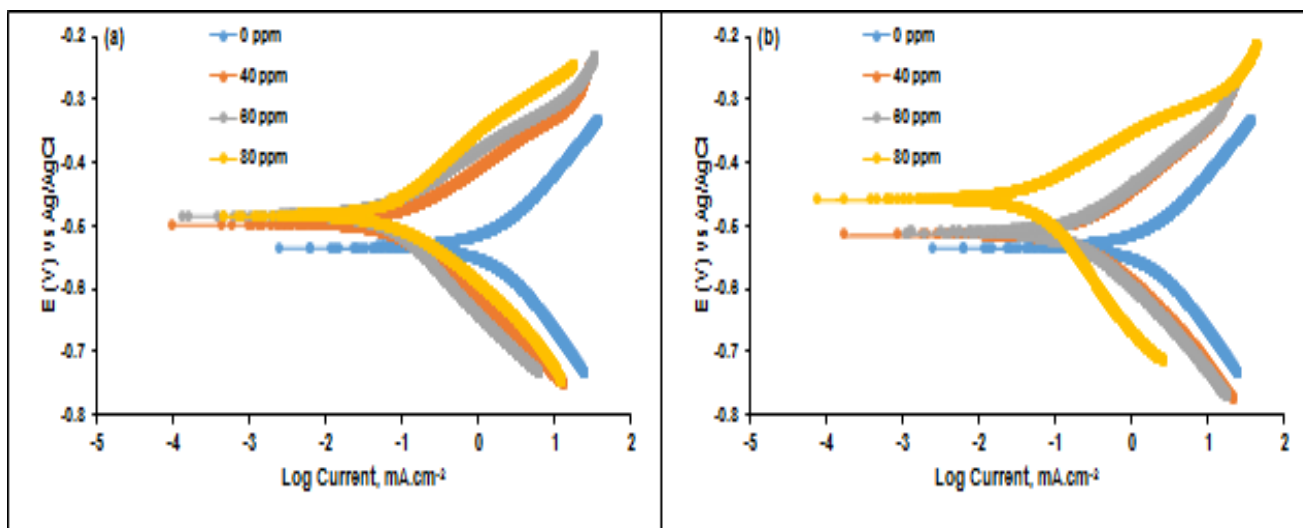


Figure 3. Potentiodynamic polarization curves of aluminium in 1 M HCl in the absence and presence of different concentrations of CuPc (a) and TNCuPc (b) inhibitor compounds.

Table 1. Corrosion potential (E_{corr}), corrosion current density (i_{corr}), anodic Tafel slope (b_a), cathodic Tafel slope (b_c), passive current density (i_{pas}) and passivation potential (E_{pas}) parameters obtained from PDP measurements using CuPc and TNCuPc inhibitors.

Inhibitor	Conc. (ppm)	$-E_{\text{corr}}$ (V)	i_{corr} (mA.cm ⁻²)	b_a (V/dec)	b_c (V/dec)	$-E_{\text{pas}}$ (V)	i_{pas} (mA.cm ⁻²)	IE_{PDP} (x 10 ² %)
Blank		0.534	1.940	0.155	0.180	0.465	4.677	-
CuPc	40	0.499	0.091	0.083	0.114	0.380	2.455	0.953
	60	0.485	0.061	0.079	0.128	0.331	1.905	0.969
	80	0.486	0.024	0.079	0.106	0.322	1.738	0.988
TNCuPc	40	0.515	0.260	0.109	0.125	0.412	2.188	0.866
	60	0.512	0.130	0.093	0.108	0.400	2.754	0.933
	80	0.459	0.040	0.068	0.144	0.334	2.249	0.979

3.2.2. Electrochemical impedance spectroscopy (EIS)

The most essential information obtained from the EIS measurements is insight about the metal corrosion behaviour against time of the metal and inhibitors. The impedance spectra of aluminium metal in 1 M HCl in the presence and absence of various concentrations of CuPc and TNCuPc are presented as Nyquist plots. The Nyquist plots are characterized by the capacitive loop related to the charge transfer process and double layer capacitance (C_{dl}) [50]. As presented in Fig. 4, a capacitive like-loop which varies with different inhibitors, and the mechanism of the corrosion inhibition process can be determined. A considerable increase in the total impedance was noticeable upon the addition of both CuPc and TNCuPc inhibitors. In the presence of CuPc, the semicircle of the uninhibited system has a lower diameter as compared to the inhibited system, and the least inhibitor concentration (40 ppm) shows the least diameter as compared to the highest inhibitor concentration (80 ppm). The increase in inductive loop appeared with the addition of 80 ppm CuPc in acid solution, which shows the reaction of double electric layer at the interface between the acid and the electrolyte [14]. This observation is due to the formation of the adsorption film on the aluminium metal surface as well as the charge transfer. In addition, the larger semicircle diameter size indicates that the more of CuPc present in the corrosive medium results in the more rate of the formation of the adsorption film on the metal which also plays a huge role in higher inhibition efficiency values. Similar behaviour was observed in the case of TNCuPc inhibitor. However, the capacitive like-loop for TNCuPc was smaller than the one of CuPc. This behaviour may be attributed to the difference in the solubility of these two unsubstituted CuPc and nitro substituted CuPc and the steric hindrance provided by the presence of NO₂. This will result in an unstable system and induce complex electrochemical behavior.

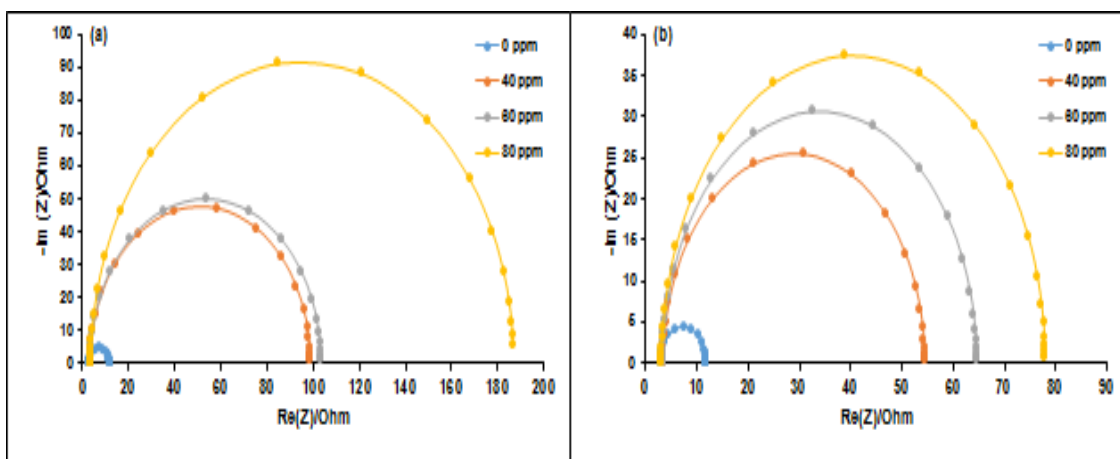


Figure 4. Nyquist plot of aluminium in 1 M HCl in the absence and presence of different concentrations of CuPc (a) and TNCuPc (b) inhibitor compounds.

Fig. 5 depicts the equivalent Randle circuit used to fit the impedance semicircles data resulting in the EIS kinetic parameters such as the solution resistance (R_s) charge transfer resistance (R_{ct}) and C_{dl} recorded in Table 2. The inhibition efficiency ($\%IE_{EIS}$) was computed from the charge transfer resistance using the (Eq. 2) below:

$$\%IE_{EIS} = \left(\frac{R'_{ct} - R_{ct}}{R'_{ct}} \right) \times 100 \tag{2}$$

where R'_{ct} and R_{ct} are the charge transfer resistance of aluminium metal in the absence and presence of the inhibitor, respectively. Table 2 clearly demonstrates that the increase of R_{ct} values with increase in inhibitor concentration. The trend signifies that the surface coverage on aluminium metal by inhibitors increases due to the increased number of inhibitor molecules in the corrosive medium [51]. An increase in the value of R_{ct} results in increase in the $\%IE$ values. From the data in Table 2, it is observed that the R_s values between the working electrode and counter electrode are smaller compared to the values of R_{ct} . Furthermore, the R_s increased with increase in the concentration of CuPc and TNCuPc inhibitors, suggesting the formation of insulated adsorption layer on the surface of an aluminium metal [14]. The C_{dl} values decreased at 40 ppm CuPc and TNCuPc inhibitors indicating a reduction in a local dielectric constant [20] between the metal and electrolyte induced by the adsorption of inhibitors. The descent order of $\%IE_{EIS}$ value is as TNCuPc > CuPc at different inhibitor concentration and is consistent with the $\%IE_{PDP}$ results obtained by the PDP measurements.

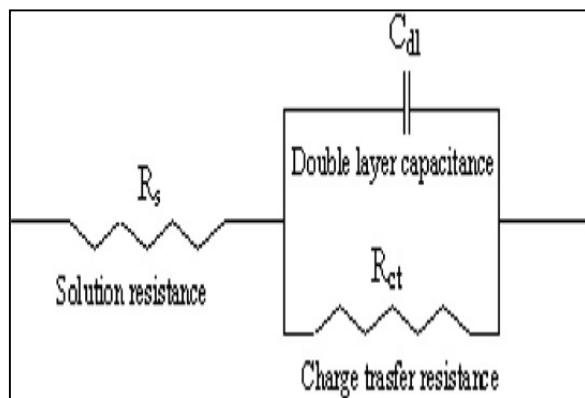


Figure 5. The suggested equivalent circuit model for the studied system.

Table 2. Impedance parameters for corrosion of aluminium in 1 M HCl containing different concentrations of CuPc and TNCuPc inhibitor.

Inhibitor	Conc. (ppm)	R_s (Ω)	R_{ct} ($\times 10^2 \Omega$)	C_{dl} ($\times 10^{-4}$ F)	IE_{EIS} ($\times 10^2$ %)
Blank		2.836	0.089	2.060	-
CuPc	40	3.245	0.955	1.210	0.907
	60	3.325	1.000	2.000	0.911
	80	3.619	1.833	2.720	0.952
TNCuPc	40	3.367	0.510	1.660	0.826
	60	3.216	0.613	1.560	0.855
	80	3.038	0.749	1.890	0.882

4. CONCLUSIONS

Phthalocyaninatocopper(II) and 4-tetranitro(phthalocyaninato)copper(II) inhibitors were successfully synthesized and confirmed by XRD, FTIR, TGA, DSC and UV-vis techniques. The crystallinity of the TNCuPc was affected by the introduction of the nitro groups compared to the unsubstituted CuPc, which resulted in an amorphous structure. The thermal stability of the CuPc was improved upon introduction of NO_2 groups on the peripheral position. The corrosion behavior of the CuPc and TNCuPc inhibitors for aluminium metal in 1 M HCl was investigated using PDP and EIS techniques. The passivation film formed on the Al metal surface was observed in both CuPc and TNCuPc by obtaining a decrease in the passivation current density and passivation potential values. The percentage of inhibition efficiency decreased with introduction of NO_2 group at peripheral position of the CuPc inhibitor due to steric hindrance. Nyquist data displayed a single capacitive and depressed loop in both CuPc and TNCuPc inhibitors indicating that the corrosion process was under the charge transfer control. It is explored and proven in this contribution that phthalocyaninatocopper(II) and its 4-tetranitro substituted counterpart can carry tremendous potential for industrial usage as corrosion inhibitors for metals.

ACKNOWLEDGEMENTS

This work was financially supported by the National Research Foundation (NRF) (Grant Nos. 99166 and 99278) and University of Limpopo (Research Development Grants R202 and R232), South Africa. MJH and KDM would also like to thank Mr T.G. Tsoeunyane at the University of Johannesburg (Doornfontein) for helping with electrochemical experiments. The Sasol Inzalo Foundation of South Africa is acknowledged for purchasing the STA instrument.

References

1. Y.F. Zheng, X.N. Gu, and F. Witte, *Mater. Sci. Eng. R. Rep.*, 77 (2014) 1.
2. P.K. Bowen, J. Drelich, and J. Goldman, *Adv. Mater.*, 25 (2013) 2577.
3. E.A. Starke, *Adv. Mater. Sci. Eng.*, 29 (1997) 99.
4. J. T. Staley, *Enc. Phys. Sci.*, 1 (1992) 591.
5. P. Arellanes-Lozada, O. Olivares-Xometl, D. Guzmán-Lucero, N.V. Likhanova, M. A. Domínguez-Aguilar, I. V. Li Janova, and E. Arce-Estrada, *Materials*, 7 (2014) 5711.
6. U. Trdan, and J. Grum, *Corros. Sci.*, 59 (2012) 324.
7. M.T. Muniandy, A.A. Rahim, H. Osman, A.M. Shah, S. Yahya, and P.B. Raja, *Surf. Rev. Lett.*, 18 (2011) 127.
8. M. Tourabi, K. Nohair, M. Traisnel, C. Jama, and F. Bentiss, *Corros. Sci.*, 75 (2013) 123.
9. S. Şafak, B. Duran, A. Yurt, and G. Türkoğlu, *Corros. Sci.*, 54 (2012) 251.
10. B. Sanyal, *Prog. Org. Coat.*, 9 (1981) 165.
11. A. Singh, Y. Lin, M.A. Quraishi, L.O. Olasunkanmi, O.E. Fayemi, Y. Sasikumar, B. Ramagathan, I. Bahadur, I.B. Obot, I.B., Adekunle, and M.M. Kabanda, *Molecules*, 20 (2015) 15122.
12. Z. Cao, Y. Tang, H. Cang, J. Xu, G. Lu, and W. Jing, *Corros. Sci.*, 83 (2014) 292.
13. L.O. Olasunkanmi, I.B. Obot, M.M. Kabanda, and E.E. Ebenso, *J. Phys. Chem. C*, 119 (2015) 16004.
14. M. Dibetsoe, L.O. Olasunkanmi, O.E. Fayemi, S. Yesudass, B. Ramagathan, I. Bahadur, A.S. Adekunle, M.M. Kabanda, and E.E. Ebenso, *Molecules*, 20 (2015) 15701.
15. C. Göl, M. Malkoç, S. Yeşilot, and M. Durmuş, *Dyes Pigm.*, 111 (2014) 81.
16. I. H. Hashim, and K. Hamzah, *J. Fiz. UTM*, 4 (2009) 56.
17. O.K. Özdemir, A. Aytaç, D. Atilla, and M. Durmuş, *J. Mater. Sci.*, 46 (2011) 752.
18. M.J. Bahrami, S.M.A. Hosseini, and P. Pilvar, *Corros. Sci.*, 52 (2010) 2793.
19. J.C. Valle-Quitana, G.F. Dominguez-Patiño, and J.G. Gonzalez-Rodriguez, *ISRN Corros.*, 2014 (2014) 1.
20. I.V. Aoki, I.C. Guedes, and S.L.A. Maranhão, *J. Appl. Electrochem.*, 32 (2002) 915.
21. A.A. Mazhar, W.A. Badaway, and M.M. Abou-Romai, *Surf. Coat. Technol.*, 29 (1896) 335.
22. A.K. Maayta, and N.A.F. Al-Rawashdeh, *Corros. Sci.*, 46 (2006) 1129.
23. M. Finsgar, and J. Jackson, *Corros. Sci.*, 86 (2014) 17.
24. E.E. Ebenso, P.C. Okafor, and U.J. Ekpe, *Anti-Corros. Methods Mater.*, 37 (2003) 381.
25. P. Zhao, Q. Liang, and Y. Li, *Appl. Surf. Sci.*, 252 (2005) 1596.
26. Z. Bıyıklıoğlu, *Synth. Met.*, 162 (2012) 26.
27. M. Arıcı, D. Arıcan, A.L. Uğur, A. Erdoğan, and A. Koca, *Electrochim. Acta*, 87 (2013) 554.
28. K.D. Modibane, and T. Nyokong, *Polyhedron*, 28 (2009) 479.
29. M.A. Abu-Dalo, N.A.F. Al-Rawashdeh, and A. Ababneh, *Desalination*, 313 (2013) 105.
30. S. Zongo, M.S. Dhlamini, P.H. Neethling, A. Yao, M. Maaza, and B. Sahraoui, *Opt. Mater.*, 50 (2015) 138.
31. C. Vergnat, V. Landais, J.F. Legrand, and M. Brinkmann, *Int. J. Biol. Macromol.*, 44 (2011) 3817.

32. A. Pick, M. Klues, A. Rinn, K. Harms, S. Chatterjee, and G. Witte, *Cryst. Growth Des.*, 15 (2015) 5495.
33. Y. Wan, S. Chen, G. Wang, Q. Liang, Z. Li, and S. Xu, *Acta Phys. Pol. A*, 130 (2016) 785.
34. X. Zhou, X. Wang, B. Wang, Z. Chen, C. He, and Y. Wu, *Sens. Actuators B*, 193 (2014) 340.
35. A.R. Koray, V. Ahsen, and Ö. Bekâroğlu, *J. Chem. Soc. Chem. Commun.*, 12 (1986) 932.
36. M. Zhang, C. Shao, Z. Guo, Z. Zhang, J. Mu, P. Zhang, T. Cao, and Y. Liu, *ACS Appl. Mater. Interfaces*, 3 (2011) 2573.
37. T.N. Rajesh, J. Keshavayya, M.N.K. Harish, R.A.S. Shoukat, and C.K.T. Kumar, *Res. J. Chem. Sci.*, 3 (2013) 36.
38. P. Kumari, N. Sinha, P. Chauhan, and MS Chauhan, *Curr. Org. Synth.*, 8 (2011) 393.
39. F.D. Cong, B. Ning, H.F. Yu, X.J. Cui, B. Chen, S.G. Cao, and C.Y. Ma, *Spectrochim. Acta A Mol. Biomol. Spectrosc.*, 62 (2005) 394.
40. A. Koca, *Electrochem. Commun.*, 11 (2009) 838.
41. R. Litran, E. Blanco, M. Ramirez-Del-Solar, and L. Esquivias, *J. Sol-Gel Sci. Technol.*, 8 (1997) 985.
42. T.H. Ibrahim, Y. Chehade, and M.A. Zour, *Int. J. Electrochem. Sci.*, 6 (2011) 6542.
43. L.C. Murulana, M.M. Kabanda, and E.E. Ebenso, *J. Mol. Liq.*, 215 (2016) 763.
44. I.B. Obot, and N.O. Obi-Egbedi, *Curr. Appl. Phys.*, 11 (2011) 382.
45. *RSC Adv.*, 5 (2015) 14804.
46. F.S. de Sousa and A. Spinelli, *Corros. Sci.*, 51(2009) 642.
47. Sudheer, and M.A. Quraishi, *Ind. Eng. Chem. Res.*, 53 (2014) 2851.
48. A.K. Maayta, and N.A.F. Al-Rawashdeh, *Corros. Sci.*, 46 (2004) 1129.
49. G.E. Badr, *Corros. Sci.*, 49 (2009) 2529.
50. H.H. Hassan, E. Abdelghani, and M.A. Amin, *Electrochim. Acta*, 52 (2007) 6359.
51. K.S. Jacob, and G. Parameswaran, *Corros. Sci.*, 52 (2010) 224.

© 2019 The Authors. Published by ESG (www.electrochemsci.org). This article is an open access article distributed under the terms and conditions of the Creative Commons Attribution license (<http://creativecommons.org/licenses/by/4.0/>).